ACS EARTH AND SPACE CHEMISTRY

http://pubs.acs.org/journal/aesccq

Article

Molecular-Level Mechanism of Phosphoric Acid Digestion of Carbonates and Recalibration of the $^{13}C-^{18}O$ Clumped Isotope Thermometer

Siting Zhang, Qi Liu, Mao Tang, and Yun Liu*

Cite This: *ACS Earth Space Chem.* 2020, 4, 420−433

Read Online

ACCESS | Metrics & More | Article Recommendations

ABSTRACT: The kinetic isotope effect (KIE) produced by the phosphoric acid digestion reaction of carbonates has been well studied since the beginning of stable isotope geochemistry, but its molecular-level mechanism remains elusive. Importantly, the validity of carbonate $^{13}C-^{18}O$ clumped isotope thermometry, which is heavily based on the phosphoric acid digestion treatment, needs further study. The existing $\Delta_{47}-T$ relationships calibrated by different groups are incompatible and create substantial confusion in the community. Here, we propose a new model of the molecular-level mechanism of the phosphoric acid digestion reaction of carbonates. This new model, which points out that there are three parallel pathways undergoing for the phosphoric acid digestion process, can explain a large part of discrepancies of the $\Delta_{47}-T$ relationships obtained by different groups in slightly different experimental conditions. Specifically, it provides different clumped isotope enrichment factors for the reaction at 25, 70, and 90 °C than previous theoretical studies. Under the absolute reference frame (ARF) treatment, these factors are important to obtain comparable $\Delta_{47}-T$ relationships. Combined with the equilibrium clumped isotope fractionation factors, which are recalculated using higher-order theoretical treatments, e.g., the anharmonic corrections, a new theoretical $\Delta_{47}-T$ relationship is built. This new relationship is no longer a single line but a range that varies to a small extent due to the changes of individual contributions of the three parallel pathways and reflects slight differences in experimental procedures and conditions. These calibration lines have a constant slope close to those of digested at 90 °C but significantly smaller than those at 25 °C. Based on linear mathematical analysis, an unknown isotope effect causing heavy O isotope enrichment during the experiments at 25 °C can be clearly identified. We speculate that this hidden factor was the cause of the rise of slopes. Using a strictly controlled experiment, the distribution of those calibration lines at 90 °C can be largely narrowed down, providing a good base for constructing an ideal clumped isotope thermometer. Extraction of CO_2 from carbonate by phosphoric acid digestion and measurement of ^{17}O in CO_2 have been used to obtain accurate ^{17}O isotope compositions in carbonate minerals. Our three-pathway mechanism model also provides good predictions of triple oxygen isotope relationships during the phosphoric acid digestion process.

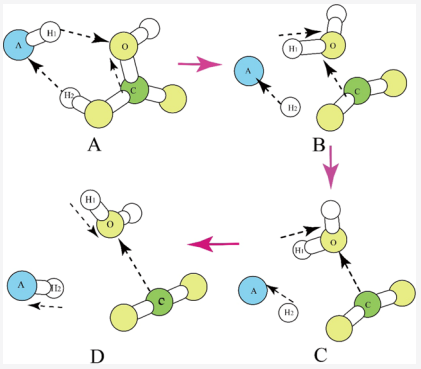

KEYWORDS: *clumped isotope, KIE, three parallel pathways, carbonates, triple oxygen isotope*

INTRODUCTION

The phosphoric acid digestion of carbonates is a common procedure for measuring oxygen isotope ($\delta^{18}O$) and $^{13}C-^{18}O$ clumped isotope compositions of carbonates, which are two important geothermometers.[1,2] It has been widely recognized that during the phosphoric acid digestion processes the produced CO_2 enriches heavy oxygen isotopes.[3−5] Since only two-thirds of the total oxygen atoms in carbonates are liberated as gaseous CO_2 during the phosphoric acid digestion, the kinetic isotope fractionation of oxygen isotopes must be considered.

Many experiments were implemented to calibrate the kinetic isotope effect (KIE) during the phosphoric acid digestion reaction.[3,6−11] Nevertheless, subtle but clear differences were observed in different experimental studies. For example, the $\delta^{18}O$ enrichment in CO_2 varied from 10.10 to 10.52‰ for calcite digestion and from 10.29 to 11.01‰ for aragonite digestion.[3,4,8,11] Besides absolute values, slopes of the $\delta^{18}O-T$ relationship also varied slightly.[10,12] Although these observed discrepancies of $\delta^{18}O$ enrichment have been discussed, there is no explanation on the perspective of molecular-level mechanism to date.[8−10]

These small discrepancies have been passed on to the new generation of geothermometry, i.e., the carbonate clumped isotope geothermometry, which is based on the concentration of two rare isotopes "clumping" (e.g., $^{13}C-^{18}O$ clumping) in

Received: November 21, 2019
Revised: January 8, 2020
Accepted: February 6, 2020
Published: February 7, 2020

https://dx.doi.org/10.1021/acsearthspacechem.9b00307
ACS Earth Space Chem. 2020, 4, 420−433

the released CO_2. The deviation of a doubly substituted isotopologue (e.g., $^{16}O^{13}C^{18}O$ in CO_2) from its random distribution, denoted "Δ_i", is proportional to its formation temperature, or due to the same mass of $^{16}O^{13}C^{18}O$, $^{17}O^{13}C^{17}O$, and $^{17}O^{12}C^{18}O$ isotopologues, the "Δ_{mass}" (i.e., Δ_{47}) is used instead.[2,12−15] The advantage of using such a geothermometer is that the information of $\delta^{18}O$ of water and the $\delta^{13}C$ of dissolved inorganic carbon (DIC) of the carbonate mineral growing environment is no longer needed. Therefore, many difficult situations in geologic processes can be circumvented.[13−17]

One of the foundations of the carbonate clumped isotope geothermometry is the calibration of the $\Delta_{47}-T$ relationship.[13,18] This relationship is needed to obtain the formation temperatures of the geological samples. Recently, a large number of carbonate clumped isotope studies have been conducted, including inorganic carbonates at known temperatures and biogenic carbonates, e.g., fish otoliths, mollusks, brachiopods, teeth, coral, and lake micritic carbonates.[13,17,19−22] Ghosh et al.[13] first suggested a $\Delta_{47}-T$ relationship using synthetic inorganic carbonate minerals at known temperatures. This relationship was then re-examined using different calcite precipitation methods.[17] However, a quite different $\Delta_{47}-T$ calibration line in terms of the intercept and slope was obtained using the absolute reference frame (ARF). The ARF is mainly used for resolving the differences of C−O bond re-ordering caused by ionization processes in instruments of different laboratories.[23] Other calibrations[24−26] using biogenic materials also showed large disagreements with the calibration line of Ghosh et al.[13] Zaarur et al.[19] re-investigated the $\Delta_{47}-T$ relationship using the same method of Ghosh et al.[13] but obtained a line with a smaller slope. Some studies suggested that the vital effect was the reason accounting for these discrepancies.[13,20,22,27] Davies and John[27] studied the vital effect of clumped isotopes in echinoid calcites using phosphoric acid digestion at 90 °C and found a positive offset of 0.014‰ in Δ_{47} relative to the inorganic calibration. They concluded that the offset could not be explained by interlaboratory differences and is a constant in the whole temperature range of species growth. This means that the vital effect cannot affect the slope of the calibration line. In addition, even samples without vital effects, e.g., synthetic inorganic carbonates, also have large discrepancies in both the intercept and slope.[13,17,19,26,28]

It has been observed that the slopes of calibrated $\Delta_{47}-T$ relationships can be grouped into three groups, i.e., digested at 25, 70, and 90 °C.[26,29−32] This seems to suggest that there is a relationship between the calibration line slope and the acid digestion temperature of carbonates. Therefore, additional experimental studies have investigated the influences of acid digestion temperature.[33−37] However, some of these studies found that the slope was insensitive to the acid digestion temperature.[34,36,37]

Another proposed explanation is the use of different ^{17}O correction parameters (Gonfiantini and Brand) for the calculation of Δ_{47}, causing such interlab discrepancies.[38,39] When using the same set of parameters (e.g., the Brand parameters), the discrepancies become smaller; however, large nonsystematic discrepancies may still exist. Löffler et al. and Kato et al. found that the choice of ^{17}O correction cannot be responsible for the large difference in the observed $\Delta_{47}-T$ calibration line.[40,41] Bernasconi et al. proposed a way to reduce the interlab discrepancies using the same suite of carbonate standards.[42] They recalculated the results of Kele et al. and compared these with those of Kelson et al. and found that the discrepancies between the two labs could be further narrowed down.[32,34] Peral et al. used carbonate standards ETH-1 to ETH-4 and further confirmed the conclusion of Bernasconi et al.[42,43] Based on this improved understanding of calibration, the ability to construct a universal calibration line in different laboratories is suggested.[33,34,42]

From the perspective of the molecular-level mechanism, spectroscopy studies suggested that carbonic acid (H_2CO_3) was produced and absorbed on the carbonate mineral surface during acid digestion.[44,45] Based on this observation, a two-step pathway for the digestion reaction was proposed.[16] First, the CO_3^{2-} ions in carbonates start to bond with H^+ to form H_2CO_3 and eventually produce a layer of H_2CO_3 on the surface of carbonate minerals. Then, the H_2CO_3 molecules dissociate into H_2O and CO_2. Based on several experimental studies, Guo et al.[16] suggested that no isotope fractionations occur in the H_2CO_3 formation step. In the second H_2CO_3-dissociation step, they used a single H_2CO_3 molecule dissociation model to simulate the isotope enrichment of Δ_{47} and $\delta^{18}O$ and found large KIEs due to the selective breaking of C−O bonds.[16] Their calculated KIEs matched well with experimental results without putting the experimental results into the ARF, i.e., considering the loss of some $^{13}C-^{18}O$ bonds due to the ionization processes. However, when the experimental results were put into the ARF, the calculated results are significantly smaller than them.[18]

Despite the inconsistency between theoretical calculation results and experimental results, a single H_2CO_3 molecule is kinetically stable at room temperature with a lifetime of about 180 000 years.[46−48] In contrast, the observed phosphoric acid digestion reactions are on the time scale of hours.

In this study, we proposed and examined a completely new molecular-level mechanism, i.e., the three-parallel-pathway (3PP) model. Our model can efficiently accelerate the acid digestion reaction. Based on this new mechanism, we recalculate all of the KIEs during the acid digestion reaction and recalibrate the $\Delta_{47}-T$ relationship in a different way.

THEORETICAL MODELS AND COMPUTATIONAL METHODS

Three-Parallel-Pathway Model. We demonstrate that the phosphoric acid digestion reaction can be effectively accelerated or catalyzed by the H-bonding. There are only three major H-containing compounds in the system, i.e., phosphoric acid (H_3PO_4), H_2CO_3, and water (H_2O). The presence of water in the system is induced by phosphoric acid that even the nominally anhydrous phosphoric acid contains a small amount of water.[30,37,49] First, the proton needed for protonation of $CaCO_3$ came from the ionization of H_3PO_4. However, this ionization process can occur only in the presence of water, which may come from the polymerization of H_3PO_4 molecules. Second, with the progress of the H_2CO_3 dissociation reaction, more and more water will be produced.

This kind of catalytic reaction has been well studied in the field of chemistry. It is called the concerted proton transfer reaction.[50] During such a reaction, two or three compounds are involved in the proton transfer processes and form a six- or eight-member ring structure. Several protons are transferred simultaneously between their reactive sites. In this way, the energy barriers of proton transfer can be kept as low as possible. Figure 1 shows the reactants and transition-state

https://dx.doi.org/10.1021/acsearthspacechem.9b00307
ACS Earth Space Chem. 2020, 4, 420−433

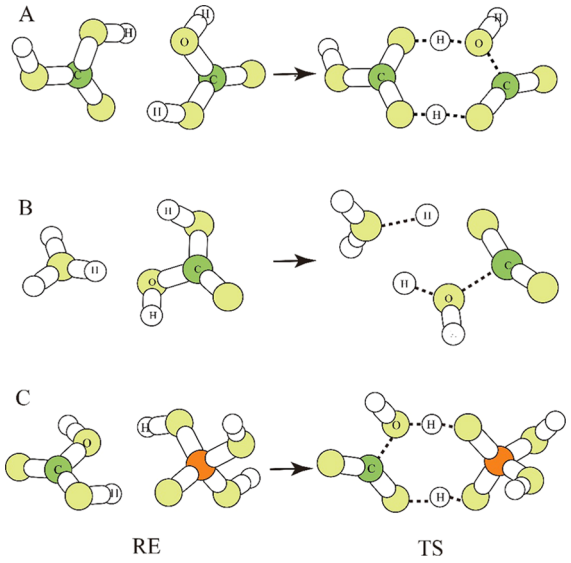

Figure 1. Optimized reactant and transition-state structures of the carbonic acid decomposition reaction. "RE" denotes the reactants, and "TS" denotes the transition-state complexes. (A) H_2CO_3-catalyzed reaction, (B) H_2O-catalyzed reaction (H_2O is as H_3O^+ under acidic conditions), and (C) H_3PO_4-catalyzed reaction.

complexes of these three different catalyzing pathways. Carbonic acid- and phosphoric acid-catalyzed pathways occur via eight-member ring structures. The water-catalyzed pathway has been investigated before, and it occurs via a six-member ring structure.[51]

Because these three reactions can take place simultaneously during the digestion process, the final result will be the sum of the individual contributions. It is therefore denoted the three-parallel-pathway mechanism model. In the later part of this paper, strict quantum chemistry calculations will reveal the kinetics of these reactions and their isotope enrichments (i.e., the KIEs). The exact activation energies of these three reactions will be calculated and compared with experimental observations.

Equilibrium Fractionation of Clumped Isotopes. The Bigeleisen−Mayer equation (hereafter, the B−M equation) or the Urey model is the foundation of stable isotope geochemistry in determining the equilibrium constant (K) of isotope exchange reactions.[52,53] According to this canonical theory, for an isotope exchange reaction between two compounds, K can be calculated from the reduced isotope partition function ratio (RPFR) of these two compounds by using only the harmonic vibrational frequencies of their isotopologues. K can be easily converted into the isotope fractionation factor α (i.e., $\alpha = K^{1/n}$ if the excess factor is ignored and n is the number of isotopes exchanged).

For the clumped isotope fractionation calculation, researchers used similar methods to compute Δ_i values.[12,14,54−56] However, there exist slightly different ways for the calculation of Δ_i. Here, we follow the definition used in Liu and Liu, and a similar definition was also used in Ono et al.[56,57] For a clumped isotope exchange reaction

$$\mathrm{A^*BX + AB^*X = A^*B^*X + ABX} \tag{1}$$

where "*" denotes a rare isotope. The equilibrium constant K of reaction 1 is

$$K_{\mathrm{A^*B^*X}} = \frac{[\mathrm{A^*B^*X}][\mathrm{ABX}]}{[\mathrm{A^*BX}][\mathrm{AB^*X}]} \tag{2}$$

or the equilibrium constant K at extremely high temperatures is

$$K^{\infty}_{\mathrm{A^*B^*X}} = \frac{[\mathrm{A^*B^*X}]^{\infty}[\mathrm{ABX}]^{\infty}}{[\mathrm{A^*BX}]^{\infty}[\mathrm{AB^*X}]^{\infty}} \tag{3}$$

where ∞ denotes the extremely high temperature. The Δ_i value of a doubly substituted isotopologue is (see the Appendix of Liu and Liu for details)[56]

$$\Delta_{\mathrm{A^*B^*X}} = \delta_{\mathrm{A^*B^*X}} - \delta_{\mathrm{A^*BX}} - \delta_{\mathrm{AB^*X}} \approx \left(\frac{K_{\mathrm{A^*B^*X}}}{K^{\infty}_{\mathrm{A^*B^*X}}} - 1\right) \times 1000 \tag{4}$$

or

$$\Delta_{\mathrm{A^*B^*X}} = \delta'_{\mathrm{A^*B^*X}} - \delta'_{\mathrm{A^*BX}} - \delta'_{\mathrm{AB^*X}} = \ln\left(\frac{K_{\mathrm{A^*B^*X}}}{K^{\infty}_{\mathrm{A^*B^*X}}}\right) \times 1000 \tag{5}$$

where $\delta' = \ln\left(\frac{R_{\mathrm{sample}}}{R_{\mathrm{reference}}}\right)$

Take the carbonate clumped isotope exchange reaction as an example

$$\mathrm{Ca^{12}C^{18}O^{16}O_2 + Ca^{13}C^{16}O_3 \leftrightarrow Ca^{13}C^{18}O^{16}O_2 + Ca^{12}C^{16}O_3} \tag{6}$$

and the equilibrium constant K can be written as

$$K_{3866} = \frac{\mathrm{RPFR(Ca^{12}C^{18}O^{16}O_2)}}{\mathrm{RPFR(Ca^{12}C^{16}O_3)}} = \frac{\mathrm{RPFR(3866/2666)}}{\mathrm{RPFR(3666/2666) \times RPFR(2866/2666)}} \tag{7}$$

where the shorthand notations denote different CO_3^{2-} isotopologues (e.g., 3866 denotes the isotopologue $^{13}C^{18}O^{16}O^{16}O^{2-}$ and 2866 denotes the isotopologue $^{12}C^{18}O^{16}O^{16}O^{2-}$). The RPFR can be expressed in terms of the harmonic normal-mode frequencies, ν_i, before and after isotope substitution[52,53]

$$\mathrm{RPFR} = \prod_i^{3n-6} \frac{u_i^* \exp(-u_i^*/2)[1 - \exp(-u_i^*)]}{u_i \exp(-u_i/2)[1 - \exp(-u_i^*)]} \tag{8}$$

and

$$u_i = \frac{h\nu_i}{kT} \tag{9}$$

where superscript "*" represents the substance with rare isotopes.

Then, the $\Delta_{^{13}C^{18}O^{16}O^{16}O}$ can be written as[56,57]

$$\Delta_{^{13}C^{18}O^{16}O^{16}O} = \ln K_{3866} \times 1000 = \ln \frac{\mathrm{RPFR(3866/2666)}}{\mathrm{RPFR(3666/2666) \times RPFR(2866/2666)}} \times 1000 \text{ (in per mil)} \tag{10}$$

Kinetic Isotope Effect Calculation. The conventional transition-state theory (TST) was originally proposed to study the chemical kinetics of an elementary step of a reaction and

https://dx.doi.org/10.1021/acsearthspacechem.9b00307
ACS Earth Space Chem. 2020, 4, 420−433

then was introduced to calculate the kinetic isotope effect of an elementary reaction.[58−60] The transition-state theory is used to estimate the rate of the chemical reaction, which can be expressed as

$$A + B \underset{k_{-1}}{\overset{k_1}{\leftrightarrow}} AB^{\neq} \overset{k_2}{\rightarrow} C + D \tag{11}$$

where A and B are the two reactants and can reversibly react to form an intermediate complex $AB^{\neq}$; if it decomposes to form the products C and D, this second step is assumed to be irreversible. The species $AB^{\neq}$ is called the transition-state complex (or the activated complex). The reaction rate of reaction 11 can be calculated by[16]

$$R = \frac{[AB^{\neq}]}{\tau} = |\nu_L^{\neq}|[AB^{\neq}] \tag{12}$$

where $[AB^{\neq}]$ denotes the concentration of the transition-state complex, τ denotes the average lifetime of the transition state, and $\nu_L^{\neq}$ denotes the "decomposition frequency" of $AB^{\neq}$.

For the H_2CO_3 dissociation, the C−O bond breaking controls the isotope fractionations. H_2CO_3 has three different isotopologues (Figure 2). The C−O bond breaking rate is different among different isotopomers. The rate ratio of different isotopologues (for the case of $^1H_2{}^{12}C^{18}O^{16}O_2$) can be expressed as[12,14]

$$R_{^{12}C^{18}O^{16}O-H_2{}^{12}C^{18}O^{16}O^{16}O}:R_{^{12}C^{18}O^{16}O-H_2{}^{12}C^{16}O^{18}O^{16}O}:R_{^{12}C^{16}O^{16}O-H_2{}^{12}C^{16}O^{16}O^{18}O}$$
$$= (|\nu_L^{\neq}| \times Q^{\neq})_{H_2{}^{12}C^{18}O^{16}O^{16}O^{\neq}}:(|\nu_L^{\neq}| \times Q^{\neq})_{H_2{}^{12}C^{16}O^{18}O^{16}O^{\neq}}:(|\nu_L^{\neq}| \times Q^{\neq})_{H_2{}^{12}C^{16}O^{16}O^{18}O^{\neq}} \tag{13}$$

where $Q^{\neq}$ is the partition function of the transition state $AB^{\neq}$

The abundances of all CO_2 isotopologues at different temperatures can be calculated using the method of Wang et al.[12] The carbonate clumped isotope thermometry is based on Δ_{47} (in per mil), which is defined by[12]

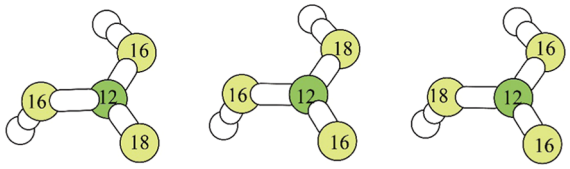

Figure 2. Three isotopomers of $^1H_2{}^{12}C^{18}O^{16}O_2$.

$$\Delta_{47} = \left(\frac{R^{47}_{actual}}{R^{47}_{random}} - 1\right) \times 1000$$
$$= \left(\frac{\frac{[^{13}C^{18}O^{16}O] + [^{12}C^{18}O^{17}O] + [^{13}C^{17}O^{17}O]}{[^{12}C^{16}O^{16}O]}}{\frac{[^{13}C^{18}O^{16}O]_r + [^{12}C^{18}O^{17}O]_r + [^{13}C^{17}O^{17}O]_r}{[^{12}C^{16}O^{16}O]_r}} - 1\right) \times 1000 \tag{14}$$

where R is the ratio of mass 47 to mass 44 in CO_2; the subscripts "actual" and "random" are actual distribution and random distribution, respectively; and the subscript "r" denotes random distribution.

The equilibrium clumped isotope fractionation of carbonate ions is defined as Δ_{63} (eq 10). The clumped isotope enrichment in the product of CO_2 due to the KIEs associated with the phosphoric acid digestion is denoted Δ^*_{47}.[16]

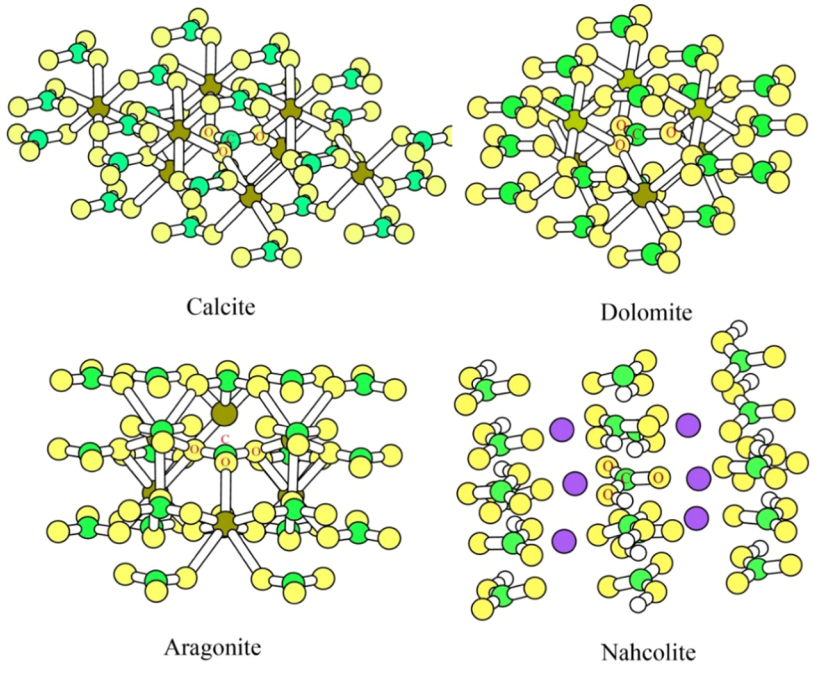

Figure 3. Cluster models used for calcite, aragonite, dolomite, and nahcolite. The $[CO_3^{2-}]$ unit at the central place of the cluster is the atom of interest.

https://dx.doi.org/10.1021/acsearthspacechem.9b00307
ACS Earth Space Chem. 2020, 4, 420−433

$$\Delta_{47}^{*} = \Delta_{47} - \Delta_{63} \quad (15)$$

The enrichment of ^{18}O in the product CO_2 is defined as $1000 \ln \alpha^*$[16]

$$1000 \ln \alpha^* = 1000 \ln \frac{\delta^{18}O_{CO_2}/1000 + 1}{\delta^{18}O_{XCO_3}/1000 + 1} \quad (16)$$

where $\delta^{18}O_{CO_2}$ is the $\delta^{18}O$ of the product CO_2 and $\delta^{18}O_{XCO_3}$ is the $\delta^{18}O$ of the carbonate reactant.

Computational Quantum Chemistry Methods. Ab initio and first-principles quantum chemistry methods have been widely used to calculate the isotope fractionation factors due to their good predictions of harmonic vibrational frequencies.[14,61−67] Usually, it is necessary to choose a frequency scale factor to improve the accuracy of such calculations.[68] However, the scaling factor is for matching pure harmonic frequencies instead of fundamental experimental frequencies when the B−M equation is used.[69]

Molecular clusters could be used to represent mineral environments.[70] The isotope effect is indeed a local effect and mostly affected by the next-nearest neighborhood atoms (i.e., the NNN rule). With a cluster size larger than this requirement, the isotope effect of the atom of interest can be properly addressed. Recently, by following the idea of Liu and Tossell and Rustad et al., we developed a modified cluster-model-based method named the volume-variable-cluster-model (VVCM) method.[62,65,67,71−73] This method can employ high-level theoretical calculations for solids. A few difficult issues, such as H-bonding in minerals, weak interactions, anharmonic effects, etc., can be addressed by the VVCM method.

In the VVCM method, the initial structure of a cluster model is built using the X-ray or neutron diffraction data of carbonate minerals under ambient pressures (e.g., from the American Mineralogist Structure Database: http://rruff.geo.arizona.edu/AMS/amcsd.php) (Figure 3). The interesting atom of study is located at the center of the clusters. The broken bonds at the outermost places of the cluster model are saturated using hundreds of virtual charge points. These virtual charge points are employed to maintain the electronic neutrality of the whole cluster and to constrain the positions of those outermost anion atoms.

The VVCM method is proposed to improve a similar method suggested by Rustad et al.[67] The largest difference between them is that a fixed layer of atoms in the model of Rustad et al. is removed, and all of the atoms in VVCM are freely optimized. This treatment is used to remedy possible false tensions produced by the fixed-volume treatment and the use of different theoretical levels for the aqueous solution and the solid phase. Under the VVCM treatment, the whole cluster is freely optimized to the lowest energy point by adjusting the positions of virtual charge points and the same theoretical level is used for both the aqueous solution and the solid.

There are a few shortcomings of the VVCM method. First, it cannot deal with situations at higher pressures other than the ambient condition. Second, the frequencies obtained by this method violate the Teller−Redlich product rule due to the outmost atoms of the cluster model bound to virtual charge points.[74] Domagal-Goldman and Kubicki suggested that the violation of the Redlich−Teller product rule might be caused by the improper molecular masses from their implicit solvent model, which possess a "no mass" or "zero mass" part.[75] The VVCM method also has a zero-mass virtual point charge part.

The errors of the violation of Redlich−Teller product rule due to the employment of the VVCM method have been checked in Gao et al.[73] It was demonstrated that if the cluster model is sufficiently large, such a violation can only bring insignificant influence on the isotope fractionation results if the atom of interest is located at the center of the cluster. Our cluster models for calcite, aragonite, dolomite, and nahcolite are all sufficiently large (Figure 3), and the atoms of interest (C−O) are all located at the center of the cluster. Their bond-length predictions are also very reasonable (Table 1).

Table 1. Comparisons of Bond Lengths between the Results of VVCM and Experiments

	exp. (Å)	VVCM (this study) (Å)	mismatch degree (%)
calcite			
Ca−O	2.359	2.366	0.3
C−O	1.284	1.286	0.1
aragonite			
Ca−O	2.528	2.535	0.3
C−O	1.287	1.285	0.09
dolomite			
Ca−O	2.381	2.386	0.2
C−O	1.287	1.284	0.2
Mg−O	2.081	2.089	0.4
nahcolite			
Na−O	2.437	2.445	0.3
C−O	1.290	1.290	0.04

The hybrid B3LYP/6-311G(d) level DFT method is used to optimize the geometries and to calculate harmonic frequencies of several important carbonate minerals, including calcite, aragonite, dolomite, and nahcolite.[76,77] For the hydrogen-containing compounds (e.g., nahcolite), an extra set of p functions is added. We find that when dealing with H-bonding in crystals, the VVCM method is particularly good.

Because metal ions in carbonate mineral crystals have only a very weak influence on the isotope fractionation of doubly substituted isotopologues, an isolated CO_3^{2-} ion is used to check the anharmonic effect on the calculation of Δ_{63} values.[14] The MP2/aug-cc-pVTZ level is chosen for the anharmonic effect calculation according to previous suggestions.[56,69]

For the phosphoric acid digestion reaction, the B3LYP/6-311+G(d,p) level is also chosen for geometry optimization and vibrational frequency calculations. By comparing the calculated harmonic frequencies between B3LYP/6-311+G(d,p) and MP2/aug-cc-pVTZ, a scaling factor (0.9949) is used to improve the results of the B3LYP/6-311+G(d,p) level. The STQN (synchronous transit-guided quasi-Newton) method (i.e., QST3) is used for transition-state complex searching. Gaussian09 software package is used for all calculations.[78]

RESULTS AND DISCUSSION

Equilibrium Clumped Isotope Fractionations in Carbonate Minerals. The final Δ_{47} value is the sum of the equilibrium $^{13}C-^{18}O$ clumping signal (Δ_{63} value) inherited from the carbonate formation at a certain temperature and the isotope enrichment (i.e., KIE) from the phosphoric acid digestion reaction. Here, we investigate the equilibrium clumped isotope fractionation first.

https://dx.doi.org/10.1021/acsearthspacechem.9b00307
ACS Earth Space Chem. 2020, 4, 420−433

Table 2. Equilibrium Δ_{63}-Value-Based Harmonic Calculation Using the VVCM Method (‰) and the Comparison with Schauble et al.[14] and Hill et al.[55]

	0 °C		25 °C			100 °C	
minerals	this study	Schauble et al.[14]	this study	Schauble et al.[14]	Hill et al.[55]	this study	Schauble et al.[14]
calcite	0.519	0.490	0.437	0.410	0.394	0.268	0.247
aragonite	0.532	0.513	0.448	0.430		0.273	0.260
dolomite	0.518	0.484	0.437	0.406		0.268	0.245
nahcolite	0.540	0.490	0.454	0.410		0.280	0.247

The temperature dependences of equilibrium clumped isotope fractionations of calcite, aragonite, dolomite, magnesite, witherite, and nahcolite, using the first-principles DFT method and lattice dynamics, have been calculated previously.[14] At 25 °C, the $[^{13}C^{18}O^{16}O_2^{2-}]$ group had a ~0.4‰ deviation from its random distribution. There were negligible variations (i.e., less than 0.03‰) among different carbonate minerals. Since the data of Schauble et al. are the only existing set of data for carbonate minerals so far, there is a desire to obtain another set of data to confirm it.[14] Here, we provide a new set of data using the VVCM method for calcite, aragonite, dolomite, and nahcolite.

Table 1 shows the bond-length comparisons between the results of the VVCM method and those from experiments. The calculated average C−O, Ca−O, and Mg−O bond lengths and the C−C distance (i.e., diagonal distance) are all in good agreement with the measured crystal structures of carbonate minerals.[79,80] Optimized geometries of calcite, aragonite, dolomite, and nahcolite (Figure 3) are used to further obtain their vibrational harmonic frequencies. No imaginary frequencies are found for all of the cluster models of the above minerals, suggesting that their structures have been optimized to energy minimum points. Then, the B−M equation is used to calculate a series of equilibrium isotope fractionation constants, as described in the Theoretical Models and Computational Methods section.

There are three different ^{18}O substitutions for the $[CO_3^{2-}]$ unit in a carbonate mineral. We used the averaged value of all of the three substitutions to obtain the equilibrium constant K_{3866}. This treatment is especially necessary for nahcolite ($NaHCO_3$), in which O atoms are under quite different chemical environments. The equilibrium constants (K_{3866}) can be approximately treated as the Δ_{63} value

$$\Delta_{63} \approx 1000 \ln K_{3866} \quad (17)$$

Table 2 shows the equilibrium Δ_{63} values from 0 to 50 °C for several carbonate minerals based on the VVCM method. For example, at 25 °C, Δ_{63} values for calcite, aragonite, dolomite, and nahcolite are 0.436, 0.445, 0.437, and 0.454‰, respectively. These results are larger than those of Schauble et al., with a difference from ~0.02 to 0.03 ‰, which is possibly caused by the different ways of the frequency scaling treatment.[14] Hill et al. calculated the Δ_{63} value of calcite using a cluster model method.[55] Their result is 0.394‰ at 25 °C and relatively smaller than the results of Schauble et al. and ours in this study.[14] This is likely due to the fixation atoms at the outer part of the cluster model, similar to that of Rustad et al.[55,67]

Our harmonic frequencies are not scaled to fundamental experimental frequencies, as Schauble et al. did.[14] On the one hand, it may be improper to scale the calculated harmonic frequencies to the experimental fundamentals because only pure harmonic frequencies are required by the B−M equation.[69] On the other hand, if our harmonic frequencies are not scaled, their accuracy is not guaranteed. Because the experimental fundamentals are the net results of harmonic frequencies minus the anharmonic contributions, if the anharmonic effects are small, then the harmonic frequencies will be very close to the experimental fundamentals, and vice versa. Therefore, the anharmonic effects are the key to help determine the accuracy of harmonic frequencies. We find that the frequencies of several isotope-effect-related vibrational modes (e.g., the C−O stretching mode) in carbonates between our calculated results and the experimental fundamentals are similar. Our results are only slightly larger than the experimental fundamentals. Meanwhile, we find that the anharmonic effects on the CO_3^{2-} unit are quite small (shown below). Therefore, our calculated frequencies are very reasonable and we choose no scaling at all. The consequence is that our equilibrium Δ_{63} results are marginally larger than those of Schauble et al.[14]

Another obvious discrepancy existing between the results of Schauble et al. and our study is that of nahcolite ($NaHCO_3$).[14] At 25 °C, their Δ_{63} value of nahcolite is the same as the value of calcite (i.e., 0.41 vs 0.41‰). However, our calcite and nahcolite results are the ones with the largest difference (i.e., 0.436 vs 0.454‰) among all studied carbonate minerals. Considering the structural and compositional differences between calcite and nahcolite, it is not likely that they have the same Δ_{63} value. The results of carbonate-ion-bearing "gaseous species" can be used to support our results indirectly. The Δ_{63} values of CO_3^{2-}, HCO_3^-, and H_2CO_3 increase one by one following the order and thus the Δ_{63} value of nahcolite is expected to be larger than that of calcite, which is consistent with our results. The pseudopotential-based methods used by Schauble et al. might have difficulty in precisely dealing with H-bearing crystalline materials.[14]

Meanwhile, our results show the similarity of Δ_{63} values between different carbonate minerals (with variations less than 0.028‰ at 25 °C), in agreement with what Schauble et al. concluded (i.e., within 0.03‰).[14] Previous studies also suggested that even an isolated CO_3^{2-} ion in the gas phase would have a K_{3866} value very similar to those in carbonates.[54] Therefore, it is confirmed that different metal ions in carbonate minerals may have a trivial influence on equilibrium C−O clumped isotope signals.

We also estimated the higher-order anharmonic corrections for carbonate minerals. Due to the "local" nature of the C−O clumped isotope effects, as described above, we choose to use an isolated CO_3^{2-} ion only to check the possible anharmonic effects.[14,54] Although the CO_3^{2-} ion is not a "real" carbonate mineral, we can obtain information about the possible magnitude of anharmonic effects. The anharmonic corrections on the Δ_{63} value are calculated at the MP2/aug-cc-pVTZ level, and our results are shown in Figure 4. The calculation details are quite cumbersome and referred to Liu et al. and Liu and Liu.[56,69] We find that the inclusion of anharmonic effects will

https://dx.doi.org/10.1021/acsearthspacechem.9b00307
ACS Earth Space Chem. 2020, 4, 420−433

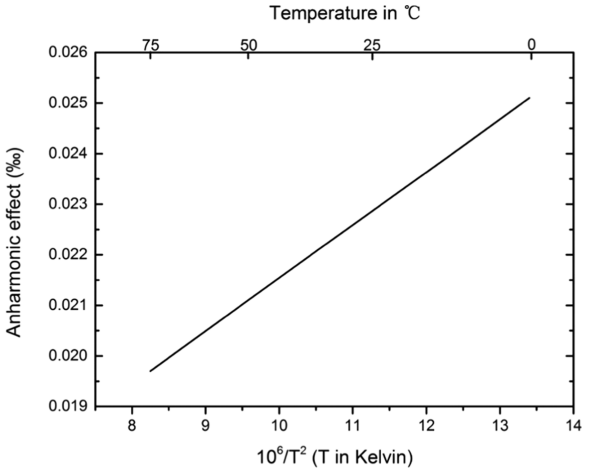

Figure 4. Anharmonic isotope effects predicted for CO_3^{2-} at the MP2/aug-cc-pVTZ level.

bring an increase of 0.023‰ to the Δ_{63} value at 298.15 K. The magnitude of the anharmonic correction on Δ_{63} is similar to a recently reported value (0.022‰) on Δ_{47} for gaseous CO_2 based on a path-integral Monte Carlo calculation via using high-quality potential energy surfaces.[81] Wang et al. also predicted that anharmonic correction on Δ_{47} for gaseous CO_2 was about 0.020‰, which is comparable to our result.[12] According to our previous work, it is reasonable to conclude that the magnitude of the anharmonic correction on the Δ_{63} value is within the range of 0.01−0.03‰ at 298.15 K.[54,56,69] Therefore, the anharmonic correction is very small and on the same order of the effect caused by different metal ions.

Considering anharmonic corrections, the new $\Delta_{63}-T$ relationships of carbonate minerals are obtained (see Figure 5). At 25 °C, Δ_{63} values for calcite, aragonite, dolomite, and

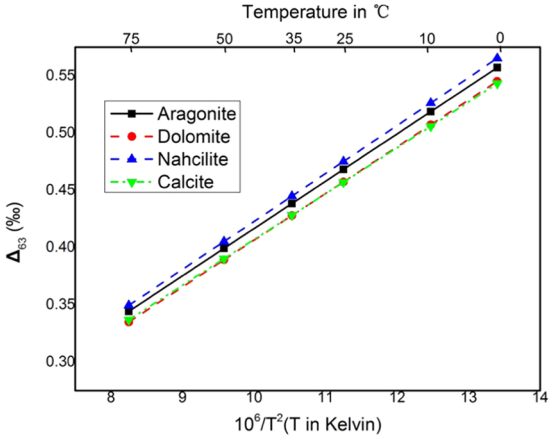

Figure 5. Calculated equilibrium Δ_{63} values of calcite, aragonite, dolomite, and nahcolite with anharmonic corrections.

nahcolite are 0.459, 0.468, 0.460, and 0.477‰, respectively. The following $\Delta_{63}-T$ relationships can be used to calculate Δ_{63} values at different temperatures

$$\Delta_{63(\text{calcite or dolomite})} = 42.7/T^2 + 0.99998 \quad (18)$$

$$\Delta_{63(\text{aragonite})} = 43.5/T^2 + 0.99998 \quad (19)$$

$$\Delta_{63(\text{nahcolite})} = 44.4/T^2 + 0.99998 \quad (20)$$

where eq 18 is for calcite and dolomite, eq 19 is for aragonite, and eq 20 is for nahcolite.

KIEs in Phosphoric Acid Digestion Processes. The activation energies and transition-state structures for the carbonic acid dissociation reaction had been calculated previously at CCSD(T)/cc-pVQZ and CCSD(T)/aug-cc-pVDZ levels.[47] Their results suggest that although the cis−trans carbonic acid is not the most stable configuration among the cis−cis, cis−trans, and trans−trans conformers, it is the most important one for the dissociation reaction of a single H_2CO_3 molecule to produce carbon dioxide. The calculated dissociation barriers of the cis−trans conformer at CCSD(T)/cc-pVQZ and CCSD(T)/aug-cc-pVDZ levels are 51.29 and 51.28 kcal/mol, respectively. These results suggest that the isolated carbonic acid molecule (H_2CO_3) is kinetically stable with a predicted lifetime of 180 000 years at room temperature.

Previous studies showed that the lifetime of H_2CO_3 decreased rapidly when it coexists with water.[48] The activation energies for the catalyzed pathways are much smaller due to the concerted proton transfer reaction. At 25 °C, our calculated activation energies are 10.7 kcal/mol for the H_2CO_3-catalyzed reaction, 11.2 kcal/mol for the H_3PO_4-catalyzed reaction, and 17.48 kcal/mol for the H_2O-catalyzed reaction at the B3LYP/6-311+G(d,p) level (Figure 6). Importantly, the activation energies of these three catalyzed pathways are close to each other, suggesting that they are all feasible pathways.

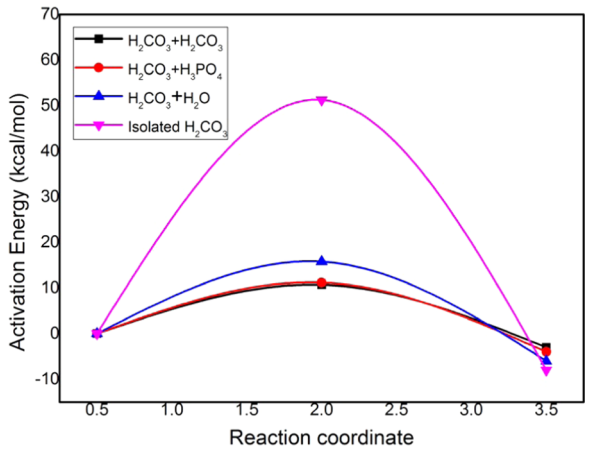

Figure 6. Calculated reaction energy profiles of the transition state for the dissociation of cis−cis H_2CO_3 to CO_2 and H_2O via isolated or three different catalyzed pathways.

Based on the calculation methods described in eqs 15 and 16, we can calculate the heavy isotope enrichments of CO_2 due to the KIEs in the phosphoric acid digestion reaction. Because of the three parallel pathways, our model produces three sets of data for both the clumped isotope and $\delta^{18}O$ enrichments (Figures 7 and 8). The $\delta^{18}O$ enrichment ($1000 \ln \alpha^*$) in the product CO_2 is 6.99, 7.39, or 15.94‰ for the H_2CO_3-, H_3PO_4-, or H_2O-catalyzed pathway, respectively, at 25 °C (Figure 7). The Δ_{47}^* values are 0.169, 0.236, and 0.301‰ for H_2CO_3-, H_3PO_4-, and H_2O-catalyzed pathways, respectively (Figure 8). The calculated $1000 \ln \alpha^*$ and Δ_{47}^* values at different temperatures can be described as

$$1000 \ln \alpha^*_{(H_2O-\text{catalyzed})} = 1.079 \times 10^6/T^2 + 3.800 \quad (21)$$

https://dx.doi.org/10.1021/acsearthspacechem.9b00307
ACS Earth Space Chem. 2020, 4, 420−433

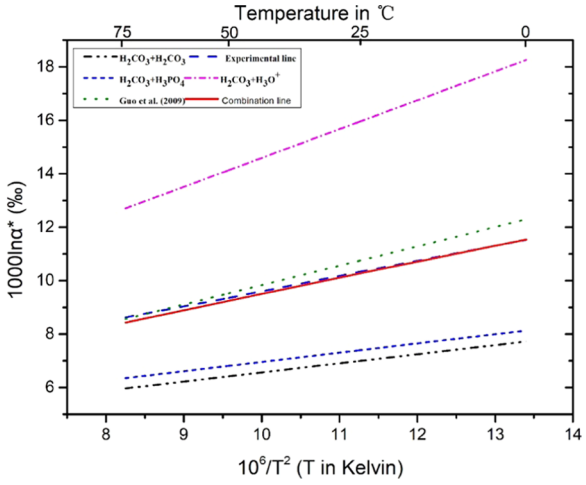

Figure 7. Oxygen isotope enrichment ($1000 \ln \alpha^*$) during phosphoric acid digestion under different pathways. The combination line is the net result of the three parallel pathways. The experimental line is from Kim et al.[10]

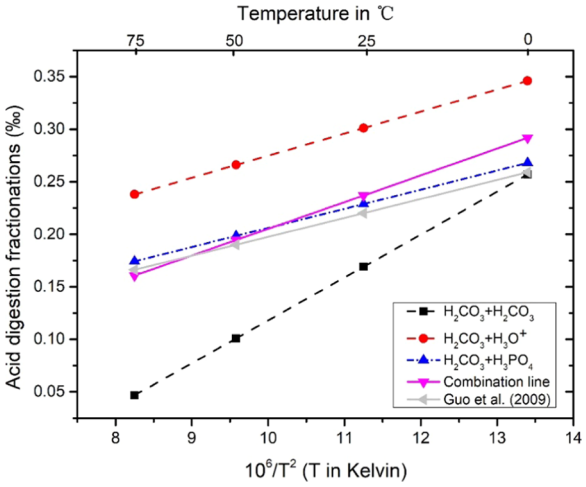

Figure 8. Δ^*_{47} values ($\Delta^*_{47} = \Delta_{47} - \Delta_{63}$) of CO_2 by different pathways and the comparison with Guo et al.[16] The combination lines are possible net results of the 3PP contributions.

$$1000 \ln \alpha^*_{(H_2CO_3-\text{catalyzed})} = 0.3409 \times 10^6/T^2 + 3.151 \quad (22)$$

$$1000 \ln \alpha^*_{(H_3PO_4-\text{catalyzed})} = 0.3465 \times 10^6/T^2 + 3.489 \quad (23)$$

$$\Delta^*_{47\ (H_2O-\text{catalyzed})} = 0.0255 \times 10^6/T^2 + 0.0045 \quad (24)$$

$$\Delta^*_{47\ (H_2CO_3-\text{catalyzed})} = 0.0449 \times 10^6/T^2 - 0.3440 \quad (25)$$

$$\Delta^*_{47\ (H_3PO_4-\text{catalyzed})} = 0.0182 \times 10^6/T^2 + 0.0241 \quad (26)$$

1000 ln α^* vs T Relationship. There have been many experimental calibrations on the $1000 \ln \alpha^*-T$ relationship of the phosphoric acid digestion process.[3,4,6,7,9,10] Figure 7 shows that there are tremendous differences in $\delta^{18}O$ enrichment (i.e., $1000 \ln \alpha^*$) among the 3PPs we proposed. At ambient temperatures, these differences can be as large as ~10‰. However, the observed spreading distributions of $\delta^{18}O$ enrichments usually are within 1‰, meaning that the change of the individual contributions is small.

Because of having almost the same activation energies and similar $\delta^{18}O$ enrichments (Figures 6 and 7), the contributions to $\delta^{18}O$ enrichments from H_2CO_3- and H_3PO_4-catalyzed pathways are similar. The contribution change of the H_2O-catalyzed pathway is therefore crucial. Consequently, the amount of H_2O in the system and the reaction time are obviously key factors, as shown in Wachter and Hayes.[49] Using phosphoric acid with a certain oversaturation degree, a certain amount of the sample and a certain running time are important to constrain the contribution from the H_2O-catalyzed pathway. Besides, the activation energy of the H_2O-catalyzed pathway is higher than those of H_2CO_3- and H_3PO_4-catalyzed pathways, meaning that temperature is another factor that can change the result.

With a higher contribution by the H_2O-catalyzed pathway, our model predicts that the $1000 \ln \alpha^*-T$ line will become steeper and the absolute $\delta^{18}O$ enrichment magnitude trend will be larger (Figure 7). The $1000 \ln \alpha^*-T$ calibration lines obtained by experiments of different groups have been compared in Guo et al.[16] There is a clear trend existing among those calibration lines, i.e., the ones with steeper slopes are generally with larger isotope enrichment magnitudes, agreeing well with the prediction of our model.

Individual Contributions of the 3PPs. From the analyses of the previous section, we only know that the change of the H_2O-catalyzed pathway is limited. A few studies have suggested that, although the $1000 \ln \alpha^*-T$ calibration results are varied in a small range, the "average" $1000 \ln \alpha^*$ value of calcite seems to be converged at ~10.2‰ at 25 °C.[8,10] We can use it as a calibration condition to figure out the individual proportions of the 3PP.

At 25 °C, our model suggests that the 3PP will have different enrichment effects, i.e., 6.99, 7.39, and 15.94‰. First, we can approximate the contributions from H_2CO_3-catalyzed and H_3PO_4-catalyzed pathways as the same value (7.19‰) because their activation energies and $\delta^{18}O$ enrichments are very close to each other (i.e., 6.99 vs 7.39‰). To let the sum of their enrichments be equal to 10.2‰, the individual contributions therefore are 35% for the H_2O-catalyzed pathway and 65% for the other two pathways. The latter are indistinguishable. These results confused us completely because the contribution of water is unexpectedly large until we were informed that there is an amount of water in anhydrous phosphoric acid.[49] Keisch et al. (1958)[82] measured the concentration of water in different phosphoric acid solutions and found that the amounts of water present were considerable even if the phosphoric acid concentration exceeded 100%. Defliese et al.[37] have shown the vapor pressure of H_2O to be even higher than that of phosphoric acid. Wacker et al. also confirmed this phenomenon.[30]

There is a "combination line" in Figure 7. It is the calibration result to let the sum of the individual contributions of 3PP (35 + 65%) equal to 10.2‰ at 25 °C. Under shorter running time and fewer samples, the change of the contribution from the H_2O-catalyzed pathway is expected to be small. We then assume that these proportions remained the same for the whole temperature range, probably a bold and improper assumption. However, in this way, our "combination lines" surprisingly match well the experimental results of calcite for the whole temperature range (Figure 7). The "combination line" and the "experimental line" are almost the same. They are

https://dx.doi.org/10.1021/acsearthspacechem.9b00307
ACS Earth Space Chem. 2020, 4, 420−433

with a smaller magnitude and slope than the calibration line of Guo et al.[16]

If the observed $\delta^{18}O$ enrichment is higher or lower than 10.2‰, the proportion of the H_2O-catalyzed pathway is possibly larger or smaller than 35%. For example, if the observed $\delta^{18}O$ enrichments are in the range of 10.10−10.52‰, the proportion of the contribution from the H_2O-catalyzed pathway will be roughly from 33 to 38%.[3,4,8,11] The accurate proportions of these three pathways are unfortunately unknown. Further specially designed experiments are needed to provide more information about them.

Δ_{47}^{*}−T Relationship. The Δ_{47}^{*} values are important not only for the theoretical calibrations but also for the experimental calibrations because they are needed for comparing results under different acid digestion temperatures under the absolute reference frame.[23] The only available Δ_{47}^{*} values used to date are the ones provided by Guo et al.[16] Based on the 3PP model, we can recalculate them here (details are in the previous section).

Figure 8 shows that the Δ_{47}^{*} values of 3PP are largely different from each other and with distinct temperature dependences. Equations 24−26 provide details of these Δ_{47}^{*} values. The H_2CO_3-catalyzed pathway has a much steeper slope than those of H_3PO_4-catalyzed and H_2O-catalyzed pathways. Its magnitude is also much smaller than those of the other two pathways.

The exact proportions of the 3PP are difficult to determine. We follow the treatment of the case of 1000 ln α^{*}−T even if the Δ_{47}^{*} values are completely different. These "combination line" with an arbitrary choice of proportions (e.g., 35 + 65%) is plotted in Figure 8.

In experiments, the difference between Δ_{47}^{*} (at 25 °C) and Δ_{47}^{*} (at 90 °C) is needed to compare the Δ_{47}−T calibration lines under ARF.[23] This difference cannot be precisely determined due to the lack of information on individual contributions of 3PP. If it is different from what Guo et al. suggested, the calibration lines of those digested at 90 °C will be relocated in ARF plots.[16] They can be moved up or down but in a parallel way, i.e., their slopes will not be changed.

Intercept of the Δ_{47}−T Relationships. Figure 9 shows some Δ_{47}−T calibration lines provided by different groups under the ARF.[13,14,16,19,23,26,28,55] If we use the arbitrary Δ_{47}^{*} value at 25 °C in Figure 8 in addition to our calculated Δ_{63} value, we will produce one theoretical calibration line, so-called "combination line" in Figure 9. Note that, due to the variations of individual contributions of 3PP, this theoretical calibration line can be moved up or down to an extent. Many recent studies tried to calibrate the Δ_{47}−T relationships in the different laboratories, which was attributed to the choice of ^{17}O correction or consistent carbonate-based standardization.[14,16,23,26,28,55,83,84] However, Figure 9 shows that the difference of the intercept among different laboratories still exists. Although the discrepancies become smaller, they have never disappeared. Interestingly, our slope is very close to those of Guo et al.,[16] Bernasconi et al.,[42] Kele et al.,[32] Kelson et al.,[34] Petersen et al.,[83] Peral et al.,[43] Swart et al.,[84] etc., but has an apparent difference with that of Ghosh et al.[13]

Daëron et al. found that if samples have a $\delta^{13}C$ or $\delta^{18}O$ far from the isotope composition of the reference, using different triple oxygen relationships will have a noticeable influence on the Δ_{47} value.[38] They suggested using the absolute isotopic abundance ratios and the parameters of Brand et al. to calculate the Δ_{47} value.[38,85] However, this "correction" method

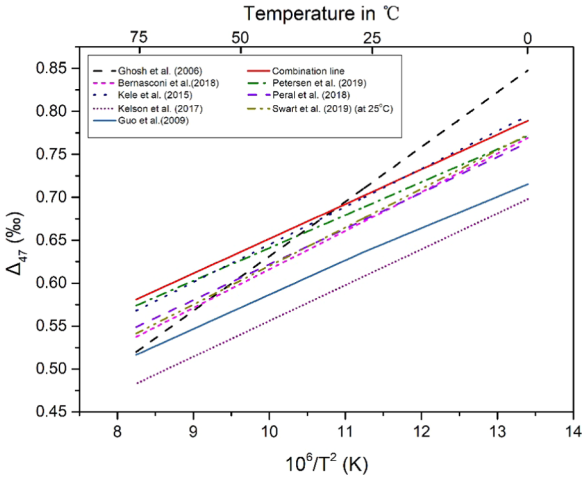

Figure 9. Comparison of calibration lines of this study, the experimental calibration lines, and the theoretical calibration line of Guo et al.[16] in ARF.[18] According to the 3PP model, the line of "this study" can be varied parallelly up or down to an extent due to the change of individual contributions.

on the Δ_{47} value may be useful only for results obtained using the same acid digestion method by the same group. Kelson et al. also found that using such "correction" treatment can bring only statistically indistinguishable differences to the results and a large part of discrepancies between different labs still exists.[34] Furthermore, Löffler et al. found no systematic difference between [Gonfiantini] and [Brand] parameterizations, which are processed with $\delta^{13}C$ ranging from −12.2 to 1.4‰ and $\delta^{18}O$ from −13.0 to 2.9‰.[40] They found that the differences of $\Delta(\Delta_{47})$ values between [Gonfiantini] and [Brand] parameterizations only range from −7 to +12 ppm, which is roughly 50% lower than those reported by Daëron et al.[38] They concluded that the different isotopic parameters played only a minor role in the discrepancies of the Δ_{47} value.[40] Similarly, Kato et al. found that the choice of ^{17}O correction has a negligible effect on the Δ_{47}−T relationship, which exhibits only a small discrepancy of 0.0083−0.0086‰ between [Santrock] and [Brand] parameters.[41] Petersen et al. had gathered 14 published clumped isotope calibration data sets to study the improved ^{17}O correction (IUPAC; Brand et al.[85]) on the temperature dependence of acid digestion fractionation.[83] They found that the IUPAC parameters showed improved agreement compared to the same data processed using SG parameters. However, they considered that there remained continued differences in the intercept, which need to be systematically investigated. Furthermore, only one of the 14 groups of publication data that they selected was acid-digested at 25 °C, while the others were acid-digested at 70−100 °C. Recently, Bernasconi et al. and Peral et al. used a common carbonate standard method to calibrate the results from different labs.[42,43] However, the discrepancies cannot be eliminated completely and thus there must be some other factors causing those discrepancies.

Our model suggests that the discrepancies among different laboratories originate from the different contributions of three pathways. Figure 10 shows the possible distribution ranges of calibration lines predicted by our 3PP model. The H_2O-catalyzed pathway offers the upper bound and the H_2CO_3-catalyzed pathway defines the lower bound of values. Therefore, any factor that affects the proportions of the three

https://dx.doi.org/10.1021/acsearthspacechem.9b00307
ACS Earth Space Chem. 2020, 4, 420−433

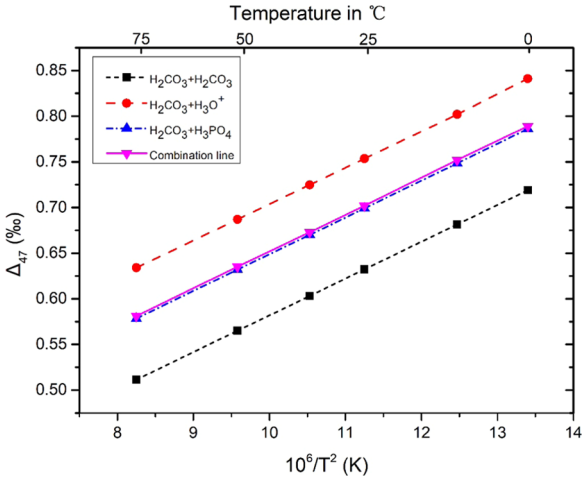

Figure 10. Possible distributions of calibration lines of the 3PP model in ARF (25 °C).

pathways will result in a different calibration line. The temperature, the amount of the sample, and the reaction time of acid digestion are three possible factors that can lead to different proportions of the 3PP. Therefore, we foresee that if all of the above factors are strictly controlled in the experiment process, the spreading distribution of calibration lines can be largely narrowed down.

Slopes of the Δ_{47} vs *T* Lines. Daëron et al. and Kelson et al. did not provide the reason for the slope change of some calibration lines based on their studies.[34,38] Our model is also unable to explain those steeper slopes among the calibration lines. However, we find that the pattern of some of the existing calibration lines resembles certain swinging lines with a common intersection point (Figure 11). Therefore, we can

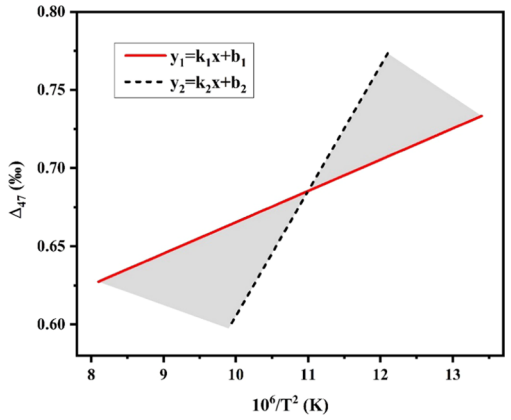

Figure 11. Schematic diagram of possible variations of the predicted slope (y_1) with different contributions from a hidden factor (y_2).

clearly identify a hidden factor that changes the slopes. Following the linear mathematical treatment, two lines with different slopes ($k_1 < k_2$) can be expressed as

$$y_1 = k_1x + b1 \tag{27}$$

$$y_2 = k_2x + b_2 \tag{28}$$

Suppose that y_1 represents the calibration line that we calculated based on the 3PP model and y_2 is the enrichment of Δ_{47} controlled by the hidden factor at different temperatures. Any final calibration result controlled by both the hidden factor and the 3PP will be a linear combination of y_1 and y_2. Symbol θ represents the proportion of y_2, and the linear combination of y_1 and y_2 can be written as

$$Y = [(1 - \Phi)k_1 + \Phi k_2)]x + b_1(1 - \Phi) + b_2 \tag{29}$$

When Φ varies with the change of experiment conditions, there will be a bunch of calibration lines produced between y_1 and y_2. Obviously, the intersection of these lines is independent of θ (Figure 11). All of them have a common intersection point. Watkins and Hunt also summed up four different calibrations of the clumped isotope thermometer and found that the curves intersect at one temperature.[86] Therefore, we can use the coordinates of the intersection point to deduce the enrichment from the hidden factor at a certain temperature, even without knowing what this hidden factor is.

Based on the analysis of the whole reaction system, we speculate that one of the possible hidden factors is the isotope exchange between CO_2 and water, resulting in the enrichment of Δ_{47}. Previous studies showed that oxygen isotope exchange occurs in the reaction of calcite with phosphoric acid, and such an exchange rate was a function of the acid digestion temperature.[6,7,49] Swart et al.[84] used identical analytical methods to study the differences between 25 and 90 °C and found that the observed difference of the slope was real. They suggested that this difference was related to the isotopic exchange between CO_2 and H_2O associated with the phosphoric acid−carbonate system.[84] At 75 °C, a significant exchange was found to occur even for the "anhydrous" phosphoric acids, those in which the concentration is equal to or exceeds 100%. If this were the case, experiments conducted at 90 °C must have been through some special treatments or arrangements to exclude the isotope exchange between CO_2 and water because their slopes are very similar to the lower bound of slopes (i.e., y_1 or our theoretical calibration line). Murray et al. also suggested that if the acid is an influencing factor for the Δ_{47}^* value, it will be very significant when the kinetic reaction is slowed (or prolonged).[87] This means that the interlaboratory difference will be reduced if all acid digestions reactions are performed at 90 °C with much shorter running time.[87] Kluge et al. indicated that if we use the absolute reference frame and perform acid digestion at 90 °C, the slope of the Δ_{47}^*-T agrees well with the predicted theoretical value.[88] Therefore, the spreading distribution of calibration lines could be narrowed down using the same experimental conditions to fix the individual contributions of the 3PP.

However, those experiments done at 25 °C seem to have involved some water exchanges or other unknown affecting factors to let their slopes rise up. Before figuring out and excluding these factors, it will be difficult to unify the results of calibration at 25 °C. The hidden factor is an important issue that needs to be further investigated. With the exclusion of the hidden factor, the calibration lines of 25 °C will be reunified with those of 90 °C.

Triple Oxygen Isotope Relationship in the Phosphoric Acid Digestion Reaction. Triple oxygen isotope compositions in carbonates hold the promise, providing additional constraints on the carbonate formation environment. To retrieve the information recorded by ^{17}O in carbonates, high-precision measurements are required. Extraction of CO_2 from carbonates by phosphoric acid digestion and

https://dx.doi.org/10.1021/acsearthspacechem.9b00307
ACS Earth Space Chem. 2020, 4, 420−433

measurement of ^{17}O in CO_2 have been used to obtain accurate ^{17}O isotope compositions in carbonate minerals.[89] However, the triple oxygen isotope fractionation during phosphoric acid digestion is just ignored in the literature, which will limit the usage of small ^{17}O anomaly recorded in carbonates and cause difficulties in interlaboratory comparison. Based on the mass-dependent fractionation relationship between ^{17}O and ^{18}O in the acid digestion process, it was assumed that the λ between them was 0.528. However, many studies found that the selection of the ^{17}O correction value for the raw data during a measurement had a very significant influence on the accuracy of the Δ_{47}.[34,38,39]

In this study, based on the 3PP model, the θ values between ^{18}O and ^{17}O during the acid digestion process of carbonates have been calculated.[66] The triple oxygen isotope fractionation relationship θ for the H_2CO_3-, H_3PO_4-, or H_2O-catalyzed pathway is found to be 0.525, 0.526, or 0.529 at 25 °C, respectively. The apparent θ between extracted CO_2 and carbonates is a function of these three intrinsic θs, and its value changes with the variation of the individual contribution. If we use the proportions found in $\delta^{18}O$ enrichment analysis as above, i.e., 35 + 65%, we can obtain the net or apparent θ as 0.527, which is very close to the assumed 0.528.[89]

CONCLUSIONS

We present equilibrium constants for the internal isotopic exchange reactions of calcite, aragonite, dolomite, and nahcolite minerals using a first-principles-based theoretical model. Our results suggest that Δ_{63} ($^{13}C^{18}O^{16}O_2^{2-}$) is around 0.46‰ in all studied carbonate minerals at 25 °C. The Δ_{63} values decrease with the increasing temperature, and there is a linear relationship between the Δ_{63} values and $1/T^2$.

The kinetic isotope effects for the phosphoric acid digestion reaction of carbonates are also calculated with a new three-parallel-pathway model. Our model provides different clumped isotope enrichment factors for the reaction at 25 and 90 °C than previous calculations. We show that the $\Delta_{47}-T$ calibration line can be varied in a small range due to the change of individual contributions of the three parallel pathways, which reflects the slightly different experimental procedures and conditions. Our calculated calibration lines also have a constant slope very close to those of digested at 90 °C but much smaller than those of digested at 25 °C. Through a linear mathematical analysis, we suggest that there is an unknown factor that can increase the slopes. This may be the reason for the discrepancies of those experiments done at 25 °C. With more strictly controlled experiments (i.e., using the same amount of samples, the same running time, the same phosphoric acid, etc.), we speculate that those calibration lines at 90 °C could be largely narrowed down and provide a reasonable $\Delta_{47}-T$ calibration line for the carbonate clumped isotope thermometry.

AUTHOR INFORMATION

Corresponding Author

Yun Liu − *State Key Laboratory of Ore Deposit Geochemistry, Institute of Geochemistry, Chinese Academy of Sciences, Guiyang 550081, China; CAS Center for Excellence in Comparative Planetology, Hefei 230026, China*; Email: liuyun@vip.gyig.ac.cn

Authors

Siting Zhang − *Center for Lunar and Planetary Science and State Key Laboratory of Ore Deposit Geochemistry, Institute of Geochemistry, Chinese Academy of Sciences, Guiyang 550081, China; CAS Center for Excellence in Comparative Planetology, Hefei 230026, China*; orcid.org/0000-0002-3551-2255

Qi Liu − *State Key Laboratory of Ore Deposit Geochemistry, Institute of Geochemistry, Chinese Academy of Sciences, Guiyang 550081, China*

Mao Tang − *State Key Laboratory of Ore Deposit Geochemistry, Institute of Geochemistry, Chinese Academy of Sciences, Guiyang 550081, China*

Complete contact information is available at: https://pubs.acs.org/10.1021/acsearthspacechem.9b00307

Notes

The authors declare no competing financial interest.

ACKNOWLEDGMENTS

Y.L. is grateful for funding support from the Strategic Priority Research Program (B) of CAS (XDB18010100) and Chinese NSF projects (41530210, 41490635). S.Z. and Q.L. are grateful to Chinese NSF projects (41773016, 41203020, 41473026).

REFERENCES

(1) McCrea, J. M. On the Isotopic Chemistry of Carbonated and a Paleotemperature Scale. *J. Chem. Phys.* **1950**, *18*, 849−857.

(2) Eiler, J. M.; Schauble, E. A. $^{18}O^{13}C^{16}O$ in Earth's atmosphere. *Geochim. Cosmochim. Acta* **2004**, *68*, 4767−4777.

(3) Sharma, T.; Clayton, R. N. Measurement of $^{18}O^{16}O$ ratios of total oxygen of carbonates. *Geochim. Cosmochim. Acta* **1965**, *29*, 1347−1353.

(4) Kim, S. T.; O'Neil, J. R. Equilibrium and nonequilibrium oxygen isotope effects in synthetic carbonates. *Geochim. Cosmochim. Acta* **1997**, *61*, 3461−3475.

(5) Zeebe, R. E. Hydration in solution is critical for stable oxygen isotope fractionation between carbonate ion and water. *Geochim. Cosmochim. Acta* **2009**, *73*, 5283−5291.

(6) Swart, P. K.; Burns, S. J.; Leder, J. J. Fractionation of the stable isotopes of oxygen and carbon in carbon-dioxide during the reaction of calcite with phosphoric-acid as a function of temperature and technique. *Chem. Geol.* **1991**, *86*, 89−96.

(7) Böttcher, M. E. $^{18}O/^{16}O$ and $^{13}C/^{12}C$ Fractionation during the reaction of carbonates with phosphoric acid: effects of cationic substitution and reaction temperature. *Isot. Environ. Health Stud.* **1996**, *32*, 299−305.

(8) Das Sharma, S.; Patil, D. T.; Gopalan, K. Temperature dependence of oxygen isotope fractionation of CO_2 from magnesite phosphoric acid reaction. *Geochim. Cosmochim. Acta* **2002**, *66*, 589−593.

(9) Gilg, H. A.; Struck, U.; Vennemann, T.; Boni, M. Phosphoric acid fractionation factors for smithsonite and cerussite between 25 and 72 °C. *Geochim. Cosmochim. Acta* **2003**, *67*, 4049−4055.

(10) Kim, S. T.; Mucci, A.; Taylor, B. E. Phosphoric acid fractionation factors for calcite and aragonite between 25 and 75 °C: Revisited. *Chem. Geol.* **2007**, *246*, 135−146.

(11) Land, L. S. *The Isotopic and Trace Element Geochemistry of Dolomite: The State of the Art*; SEPM Society for Sedimentary Geology, 1980; Vol. *28*, pp 87−110.

(12) Wang, Z. R.; Schauble, E. A.; Eiler, J. M. Equilibrium thermodynamics of multiply substituted isotopologues of molecular gases. *Geochim. Cosmochim. Acta* **2004**, *68*, 4779−4797.

(13) Ghosh, P.; Adkins, J.; Affek, H.; Balta, B.; Guo, W.; Schauble, E. A.; Schrag, D.; Eiler, J. M. $^{13}C-^{18}O$ bonds in carbonate minerals: A

new kind of paleothermometer. *Geochim. Cosmochim. Acta* **2006**, *70*, 1439−1456.
(14) Schauble, E. A.; Ghosh, P.; Eiler, J. M. Preferential formation of $^{13}C-^{18}O$ bonds in carbonate minerals, estimated using first-principles lattice dynamics. *Geochim. Cosmochim. Acta* **2006**, *70*, 2510−2529.
(15) Eiler, J. M. "Clumped-isotope" geochemistry-The study of naturally-occurring, multiply-substituted isotopologues. *Earth Planet. Sci. Lett.* **2007**, *262*, 309−327.
(16) Guo, W. F.; Mosenfelder, J. L.; Goddard, W. A.; Eiler, J. M. Isotopic fractionations associated with phosphoric acid digestion of carbonate minerals: Insights from first-principles theoretical modeling and clumped isotope measurements. *Geochim. Cosmochim. Acta* **2009**, *73*, 7203−7225.
(17) Dennis, K. J.; Schrag, D. P. Clumped isotope thermometry of carbonatites as an indicator of diagenetic alteration. *Geochim. Cosmochim. Acta* **2010**, *74*, 4110−4122.
(18) Eiler, J. M. Paleoclimate reconstruction using carbonate clumped isotope thermometry. *Quat. Sci. Rev.* **2011**, *30*, 3575−3588.
(19) Zaarur, S.; Affek, H. P.; Brandon, M. T. A revised calibration of the clumped isotope thermometer. *Earth Planet. Sci. Lett.* **2013**, *382*, 47−57.
(20) Tripati, A. K.; Eagle, R. A.; Thiagarajan, N.; Gagnon, A. C.; Bauch, H.; Halloran, P. R.; Eiler, J. M. $^{13}C-^{18}O$ isotope signatures and 'clumped isotope' thermometry in foraminifera and coccoliths. *Geochim. Cosmochim. Acta* **2010**, *74*, 5697−5717.
(21) Daëron, M.; Guo, W.; Eiler, J.; Genty, D.; Blamart, D.; Boch, R.; Drysdale, R.; Maire, R.; Wainer, K.; Zanchetta, G. $^{13}C^{18}O$ clumping in speleothems: Observations from natural caves and precipitation experiments. *Geochim. Cosmochim. Acta* **2011**, *75*, 3303−3317.
(22) Thiagarajan, N.; Adkins, J.; Eiler, J. M. Carbonate clumped isotope thermometry of deep-sea corals and implications for vital effects. *Geochim. Cosmochim. Acta* **2011**, *75*, 4416−4425.
(23) Dennis, K. J.; Affek, H. P.; Passey, B. H.; Schrag, D. P.; Eiler, J. M. Defining an absolute reference frame for 'clumped' isotope studies of CO_2. *Geochim. Cosmochim. Acta* **2011**, *75*, 7117−7131.
(24) Saenger, C.; Affek, H. P.; Felis, T.; Thiagarajan, N.; Lough, J. M.; Holcomb, M. Carbonate clumped isotope variability in shallow water corals: Temperature dependence and growth-related vital effects. *Geochim. Cosmochim. Acta* **2012**, *99*, 224−242.
(25) Eagle, R. A.; Risi, C.; Mitchell, J. L.; Eiler, J. M.; Seibt, U.; Neelin, J. D.; Li, G.; Tripati, A. K. High regional climate sensitivity over continental China constrained by glacial-recent changes in temperature and the hydrological cycle. *Proc. Natl. Acad. Sci. U.S.A.* **2013**, *110*, 8813−8818.
(26) Henkes, G. A.; Passey, B. H.; Wanamaker, A. D.; Grossman, E. L.; Ambrose, W. G.; Carroll, M. L. Carbonate clumped isotope compositions of modern marine mollusk and brachiopod shells. *Geochim. Cosmochim. Acta* **2013**, *106*, 307−325.
(27) Davies, A. J.; John, C. M. The clumped (^{13}C-^{18}O) isotope composition of echinoid calcite: Further evidence for "vital effects" in the clumped isotope proxy. *Geochim. Cosmochim. Acta* **2019**, *245*, 172−189.
(28) Tang, J.; Dietzel, M.; Fernandez, A.; Tripati, A. K.; Rosenheim, B. E. Evaluation of kinetic effects on clumped isotope fractionation (Δ_{47}) during inorganic calcite precipitation. *Geochim. Cosmochim. Acta* **2014**, *134*, 120−136.
(29) Passey, B. H.; Levin, N. E.; Cerling, T. E.; Brown, F. H.; Eiler, J. M. High temperature environments of human evolution in East Africa based on bond ordering in paleosol carbonates. *Proc. Natl. Acad. Sci. U.S.A.* **2010**, *107*, 11245−11249.
(30) Wacker, U.; Fiebig, J.; Schoene, B. R. Clumped isotope analysis of carbonates: comparison of two different acid digestion techniques. *Rapid Commun. Mass Spectrom.* **2013**, *27*, 1631−1642.
(31) Wacker, U.; Fiebig, J.; Tödter, J.; Schöne, B. R.; Bahr, A.; Friedrich, O.; Tütken, T.; Gischler, E.; Joachimski, M. M. Empirical calibration of the clumped isotope paleothermometer using calcites of various origins. *Geochim. Cosmochim. Acta* **2014**, *141*, 127−144.
(32) Kele, S.; Breitenbach, S. F. M.; Capezzuoli, E.; Meckler, A. N.; Ziegler, M.; Millan, I. M.; Kluge, T.; Dea'k, J.; Hanselmann, K.; John, C. M.; Yan, H.; Liu, Z.; Bernasconi, S. M. Temperature dependence of oxygen and clumped isotope fractionation in carbonates: a study of travertines and tufas in the 6−95 °C temperature range. *Geochim. Cosmochim. Acta* **2015**, *168*, 172−192.
(33) Katz, A.; Bonifacie, M.; Hermoso, M.; Cartigny, P.; Calmels, D. Laboratory-grown coccoliths exhibit no vital effect in clumped isotope (Δ_{47}) composition on a range of geologically relevant temperatures. *Geochim. Cosmochim. Acta* **2017**, *208*, 335−353.
(34) Kelson, J. R.; Huntington, K. W.; Schauer, A. J.; Saenger, C.; Lechler, A. R. Toward a universal carbonate clumped isotope calibration: Diverse synthesis and preparatory methods suggest a single temperature relationship. *Geochim. Cosmochim. Acta* **2017**, *197*, 104−131.
(35) Müller, I. A.; Violay, M. E. S.; Storck, J. C.; Fernandez, A.; Dijk, J. v.; Madonna, C.; Bernasconi, S. M. Clumped isotope fractionation during phosphoric acid digestion of carbonates at 70 °C. *Chem. Geol.* **2017**, *449*, 1−14.
(36) Van Dijk, J.; Fernandez; Storck, J. C.; White, T. S.; Lever, M.; Müller, I. A.; Bishop, S.; Seifert, R. F.; Driese, S. G.; Krylov, A.; Ludvigson, G. A.; Turchyn, A. V.; Lin, C. Y.; Wittkop, C.; Bernasconi, S. M. Experimental calibration of clumped isotopes in siderite between 8.5 and 62 °C and its application as paleo-thermometer in paleosols. *Geochim. Cosmochim. Acta* **2019**, *254*, 1−20.
(37) Defliese, W. F.; Hren, M. T.; Lohmann, K. C. Compositional and temperature effects of phosphoric acid fractionationon Δ_{47} analysis and implications for discrepant calibrations. *Chem. Geol.* **2015**, *396*, 51−60.
(38) Daëron, M.; Blamart, D.; Peral, M.; Affeck, H. P. Absolute isotopic abundance ratios and the accuracy of Δ_{47} measurements. *Chem. Geol.* **2016**, *442*, 83−96.
(39) Schauer, A. J.; Kelson, J.; Saenger, C.; Huntington, K. W. Choice of ^{17}O correction affects clumped isotope (Δ_{47}) values of CO_2 measured with mass spectrometry. *Rapid Commun. Mass Spectrom.* **2016**, *30*, 2607−2616.
(40) Löffler, N.; Fiebig, J.; Mulch, A.; Tütken, T.; Schmidt, B. C.; Bajnai, D.; Conrad, A. C.; Wacker, U.; Böttcher, M. E. Refining the temperature dependence of the oxygen and clumped isotopic compositions of structurally bound carbonate in apatite. *Geochim. Cosmochim. Acta* **2019**, *253*, 19−38.
(41) Kato, H.; Amekawa, S.; Kano, A.; Mori, T.; Kuwahara, Y.; Quade, J. Seasonal temperature changes obtained from carbonate clumped isotopes of annually laminated tufas from Japan: Discrepancy between natural and synthetic calcites. *Geochim. Cosmochim. Acta* **2019**, *244*, 548−564.
(42) Bernasconi, S. M.; Müller, I. A.; Bergmann, K. D.; Breitenbach, S. F. M.; Fernandez, A.; Hodell, D. A.; Jaggi, M.; Meckler, A. N.; Millan, I.; Ziegler, M. Reducing uncertainties in carbonate clumped isotope analysis through consistent 3 carbonate- based standardization. *Geochem., Geophys., Geosyst.* **2018**, *19*, 2895−20.
(43) Peral, M.; Daëron, M.; Blamart, D.; Bassinot, F.; Dewilde, F.; Smialkowski, N.; Isguder, G.; Bonnin, J.; Jorissen, F.; Kissel, C.; Michel, E.; Riveiros, N. V.; Waelbroeck, C. Updated calibration of the clumped isotope thermometer in planktonic and benthic foraminifera. *Geochim. Cosmochim. Acta* **2018**, *239*, 1−16.
(44) Al-Hosney, H. A.; Grassian, V. H. Carbonic acid: An important intermediate in the surface chemistry of calcium carbonate. *J. Am. Chem. Soc.* **2004**, *126*, 8068−8069.
(45) Al-Hosney, H. A.; Grassian, V. H. Water, sulfur dioxide and nitric acid adsorption on calcium carbonate: A transmission and ATR-FTIR study. *Phys. Chem. Chem. Phys.* **2005**, *7*, 1266−1276.
(46) Tossell, J. A. H_2CO_3 and its oligomers: Structures, stabilities, vibrational and NMR spectra, and acidities. *Inorg. Chem.* **2006**, *45*, 5961−5970.
(47) Mori, T.; Suma, K.; Sumiyoshi, Y.; Endo, Y. Spectroscopic detection of isolated carbonic acid. *J. Chem. Phys.* **2009**, *130*, No. 204308.

https://dx.doi.org/10.1021/acsearthspacechem.9b00307
ACS Earth Space Chem. 2020, 4, 420−433

(48) Loerting, T.; Bernard, J. Aqueous Carbonic Acid (H_2CO_3). *ChemPhysChem* **2010**, *11*, 2305−2309.
(49) Wachter, E. A.; Hayes, J. M. Exchange of oxygen isotopes in carbon dioxide-phosporic acid systems. *Chem. Geol.* **1985**, *52*, 365−374.
(50) Costentin, C.; Robert, M.; Savéant, J. M. Concerted proton−electron transfers: electrochemical and related approaches. *Acc. Chem. Res.* **2010**, *43*, 1019−1029.
(51) Loerting, T.; Tautermann, C.; Kroemer, R. T.; Kohl, I.; Hallbrucker, A.; Mayer, E.; Liedl, K. R. On the surprising kinetic stability of carbonic acid (H_2CO_3). *Angew. Chem., Int. Ed.* **2000**, *39*, 891−894.
(52) Bigeleisen, J.; Mayer, M. G. Calculation of equibrium constants for isotopic exchange reactions. *J. Chem. Phys.* **1947**, *15*, 261−267.
(53) Urey, H. C. The thermodynamic properties of isotopic substances. *J. Chem. Soc.* **1947**, 562−581.
(54) Cao, X. B.; Liu, Y. Theoretical estimation of the equilibrium distribution of clumped isotopes in nature. *Geochim. Cosmochim. Acta* **2012**, *77*, 292−303.
(55) Hill, P. S.; Tripati, A. K.; Schauble, E. A. Theoretical constraints on the effects of pH, salinity, and temperature on clumped isotope signatures of dissolved inorganic carbon species and precipitating carbonate minerals. *Geochim. Cosmochim. Acta* **2014**, *125*, 610−652.
(56) Liu, Q.; Liu, Y. Clumped-isotope signatures at equilibrium of CH_4, NH_3, H_2O, H_2S and SO_2. *Geochim. Cosmochim. Acta* **2016**, *175*, 252−270.
(57) Ono, S.; Wang, D. T.; Gruen, D. S.; Lollar, B. S.; Zahniser, M. S.; McManus, B. J.; Nelson, D. D. Measurement of a doubly substituted methane isotopologue, $^{13}CH_3D$, by tunable infrared laser direct absorption spectroscopy. *Anal. Chem.* **2014**, *86*, 6487−6494.
(58) Eyring, H. The activated complex and the absolute rate of chemical reactions. *Chem. Rev.* **1935**, *17*, 65−77.
(59) Eyring, H. The activated complex in chemical reactions. *J. Chem. Phys.* **1935**, *3*, 107−115.
(60) Bigeleisen, J.; Wolfsberg, M. Theoretical and experimental aspects of isotope effects in chemical kinetics. *Adv. Chem. Phys.* **1958**, *1*, 15−76.
(61) Schauble, E. A. Applying stable isotope fractionation theory to new systems. *Rev. Mineral. Geochem.* **2004**, *55*, 65−111.
(62) Liu, Y.; Tossell, J. A. Ab initio molecular orbital calculations for boron isotope fractionations on boric acids and borates. *Geochim. Cosmochim. Acta* **2005**, *69*, 3995−4006.
(63) Méheut, M.; Lazzeri, M.; Balan, E.; Mauri, F. Equilibrium isotopic fractionation in the kaolinite, quartz, water system: Prediction from first-principles density-functional theory. *Geochim. Cosmochim. Acta* **2007**, *71*, 3170−3181.
(64) Li, X. F.; Liu, Y. First-principles study of Ge isotope fractionation during adsorption onto Fe (III)-oxy hydroxide surfaces. *Chemical. Geology.* **2010**, *278*, 15−22.
(65) Li, X. F.; Liu, Y. A theoretical model of isotopic fractionation by thermal diffusion and its implementation on silicate melts. *Geochim. Cosmochim. Acta* **2015**, *154*, 18−27.
(66) Cao, X. B.; Liu, Y. Equilibrium mass-dependent fractionation relationships for triple oxygen isotopes. *Geochim. Cosmochim. Acta* **2011**, *75*, 7435−7445.
(67) Rustad, J. R.; Casey, W. H.; Yin, Q. Z.; Bylaska, E. J.; Felmy, A. R.; Bogatko, S. A.; Jackson, V. E.; Dixon, D. A. Isotopic fractionation of Mg^{2+}(aq), Ca^{2+}(aq), and Fe^{2+}(aq) with carbonate minerals. *Geochim. Cosmochim. Acta* **2010**, *74*, 6301−6323.
(68) Harris, N. J. A systematic theoretical-study of harmonic vibrational frequencies and deuterium-isotope fractionation factors for small molecules. *J. Phys. Chem. A* **1995**, *99*, 14689−14699.
(69) Liu, Q.; Tossell, J. A.; Liu, Y. On the proper use of the Bigeleisen-Mayer equation and corrections to it in the calculation of isotopic fractionation equilibrium constants. *Geochim. Cosmochim. Acta* **2010**, *74*, 6965−6983.
(70) Gibbs, G. V. Molecules as models for bonding in silicates. *Am. Mineral.* **1982**, *67*, 421−450.
(71) Liu, Y. In *On the Test of a New Volume Variable Cluster Model Method for Stable Isotopic Fractionation of Solids: Equilibrium Mg Isotopic Fractionations between Minerals and Solutions*, Goldschmidt 2013 Conference Abstracts 2013; p 1632.
(72) He, H. T.; Zhang, S. T.; Zhu, C.; Liu, Y. Equilibrium and kinetic Si isotope fractionation factors and their implications for Si isotope distributions in the Earth's surface environments. *Acta Geochim.* **2016**, *35*, 15−24.
(73) Gao, C. H.; Cao, X. B.; Liu, Q.; Yang, Y. H.; Zhang, S. T.; He, Y. Y.; Tang, M.; Liu, Y. Theoretical calculation of equilibrium Mg isotope fractionations between minerals and aqueous solutions. *Chem. Geol.* **2018**, *488*, 62−75.
(74) Redlich, O. A general relationship between the oscillation frequency of isotropic molecules (with remarks on the calculation of harmonious force constants). *Z. Phys. Chem. B* **1935**, *28*, 371−382.
(75) Domagal-Goldman, S. D.; Kubicki, J. D. Density functional theory predictions of equilibrium isotope fractionation of iron due to redox changes and organic complexation. *Geochim. Cosmochim. Acta* **2008**, *72*, 5201−5216.
(76) Becke, A. D. A new mixing of Hartree Fock and local density functional theories. *J. Chem. Phys.* **1993**, *98*, 1372−1377.
(77) Lee, C. T.; Yang, W. T.; Parr, R. G. Development of the colle-salvetti correlation-energy formula into a functional of the electron-density. *Phys. Rev. B* **1988**, *37*, 785−789.
(78) Frisch, M. J.; Trucks, G. W.; Schlegel, H. B.; Scuseria, G. E.; Robb, M. A.; Cheeseman, J. R.; Montgomery, J. A., Jr.; Vreven, T.; Kudin, K. N.; Burant, J. C.; Millam, J. M.; Iyengar, S. S.; Tomasi, J.; Barone, V.; Mennucci, B.; Cossi, M.; Scalmani, G.; Rega, N.; Petersson, G. A.; Nakatsuji, H.; Hada, M.; Ehara, M.; Toyota, K.; Fukuda, R.; Hasegawa, J.; Ishida, M.; Nakajima, T.; Honda, Y.; Kitao, O.; Nakai, H.; Klene, M.; Li, X.; Knox, J. E.; Hratchian, H. P.; Cross, J. B.; Adamo, C.; Jaramillo, J.; Gomperts, R.; Stratmann, R. E.; Yazyev, O.; Austin, A. J.; Cammi, R.; Pomelli, C.; Ochterski, J. W.; Ayala, P. Y.; Morokuma, K.; Voth, G. A.; Salvador, P.; Dannenberg, J. J.; Zakrzewski, V. G.; Dapprich, S.; Daniels, A. D.; Strain, M. C.; Farkas, O.; Malick, D. K.; Rabuck, A. D.; Raghavachari, K.; Foresman, J. B.; Ortiz, J. V.; Cui, Q.; Baboul, A. G.; Clifford, S.; Cioslowski, J.; Stefanov, B. B.; Liu, G.; Liashenko, A.; Piskorz, P.; Komaromi, I.; Martin, R. L.; Fox, D. J.; Keith, T.; Al-Laham, M. A.; Peng, C. Y.; Nanayakkara, A.; Challacombe, M.; Gill, P. M. W.; Johnson, B.; Chen, W.; Wong, M. W.; Gonzalez, C.; Pople, J. A. *Gaussian 03*, revision E.01; Gaussian, Inc.: Wallingford, CT, 2004.
(79) Ross, N. L.; Reeder, R. J. High-pressure structural study of dolomite and ankerite. *Am. Mineral.* **1992**, *77*, 412−421.
(80) Maslen, E. N.; Streltsov, V. A.; Streltsova, N. R. X-ray study of the electron-density in calcite, $CaCO_3$. *Acta Crystallogr., Sect. B: Struct. Sci.* **1993**, *49*, 636−641.
(81) Webb, M. A.; Miller, T. F. Position-Specific and Clumped Stable Isotope Studies: Comparison of the Urey and Path-Integral Approaches for Carbon Dioxide, Nitrous Oxide, Methane, and Propane. *J. Phys. Chem. A* **2014**, *118*, 467−474.
(82) Keisch, B.; Kennedy, J. W.; Wahl, A. C. The exchange of oxygen between phosphoric acid and water. *J. Am. Chem. Soc.* **1958**, *80*, 4778−4782.
(83) Petersen, S. V.; Defliese, W. F.; Saenger, C.; Daëron, M.; Huntington, K. W.; John, C. M.; Kelson, J. R.; Bernasconi, S. M.; Colman, A. S.; Kluge, T.; Olack, G. A.; Schauer, A. J.; Bajnai, D.; Bonifacie, M.; Breitenbach, S. F. M.; Fiebig, J.; Fernandez, A. B.; Henkes, G. A.; Hodell, D.; Katz, A.; Kele, S.; Lohmann, K. C.; Passey, B. H.; Peral, M. Y.; Petrizzo, D. A.; Rosenheim, B. E.; Tripati, A.; Venturelli, R.; Young, E. D.; Winkelstern, I. Z. Effects of Improved ^{17}O Correction on Inter laboratory Agreement in Clumped Isotope Calibrations, Estimates of Mineral-Specific Offsets, and Temperature Dependence of Acid Digestion Fractionation. *Geochem., Geophys., Geosyst.* **2019**, *20*, 3495−3519.
(84) Swart, P. K.; Murray, S. T.; Staudigel, P. T.; Hodell, D. A. Oxygen Isotopic Exchange Between CO_2 and Phosphoric Acid: Implications for the Measurement of Clumped Isotopes in Carbonates. *Geochem., Geophys., Geosyst.* **2019**, *20*, 3730−3750.

(85) Brand, W.; Assonov, S.; Coplen, T. Correction for the ^{17}O interference in $d^{13}C$ measurements when analyzing CO_2 with stable isotope mass spectrometry (IUPAC technical report). *Pure Appl. Chem.* **2010**, *82*, 1719−1733.
(86) Watkins, J. M.; Hunt, J. D. A process-based model for non-equilibrium clumped isotope effects in carbonates. *Earth Planet. Sci. Lett.* **2015**, *432*, 152−165.
(87) Murray, S. T.; Arienzo, M. M.; Swart, P. K. Determining the Δ_{47} acid fractionation in dolomites. *Geochim. Cosmochim. Acta* **2016**, *174*, 42−53.
(88) Kluge, T.; John, C. M.; Jourdan, A. L.; Davis, S.; Crawshaw, J. Laboratory calibration of the calcium carbonate clumped isotope thermometer in the 25−250 °C temperature range. *Geochim. Cosmochim. Acta* **2015**, *157*, 213−227.
(89) Passey, B. H.; Hua, H.; Ji, H.; Montanari, S.; Li, S.; Henkes, G. A.; Levin, N. E. Triple oxygen isotopes in biogenic and sedimentary carbonates. *Geochim. Cosmochim. Acta* **2014**, *141*, 1−25.

https://dx.doi.org/10.1021/acsearthspacechem.9b00307
ACS Earth Space Chem. 2020, 4, 420−433